ChemistryOPEN

Supporting Information

© 2018 The Authors. Published by Wiley-VCH Verlag GmbH & Co. KGaA, Weinheim

Synthesis and Application of Dendritic Fibrous Nanosilica/Gold Hybrid Nanomaterials

Wongyun Byoun, Soeun Jung, Ngoc Minh Tran, and Hyojong Yoo*[a]

open_201800040_sm_miscellaneous_information.pdf

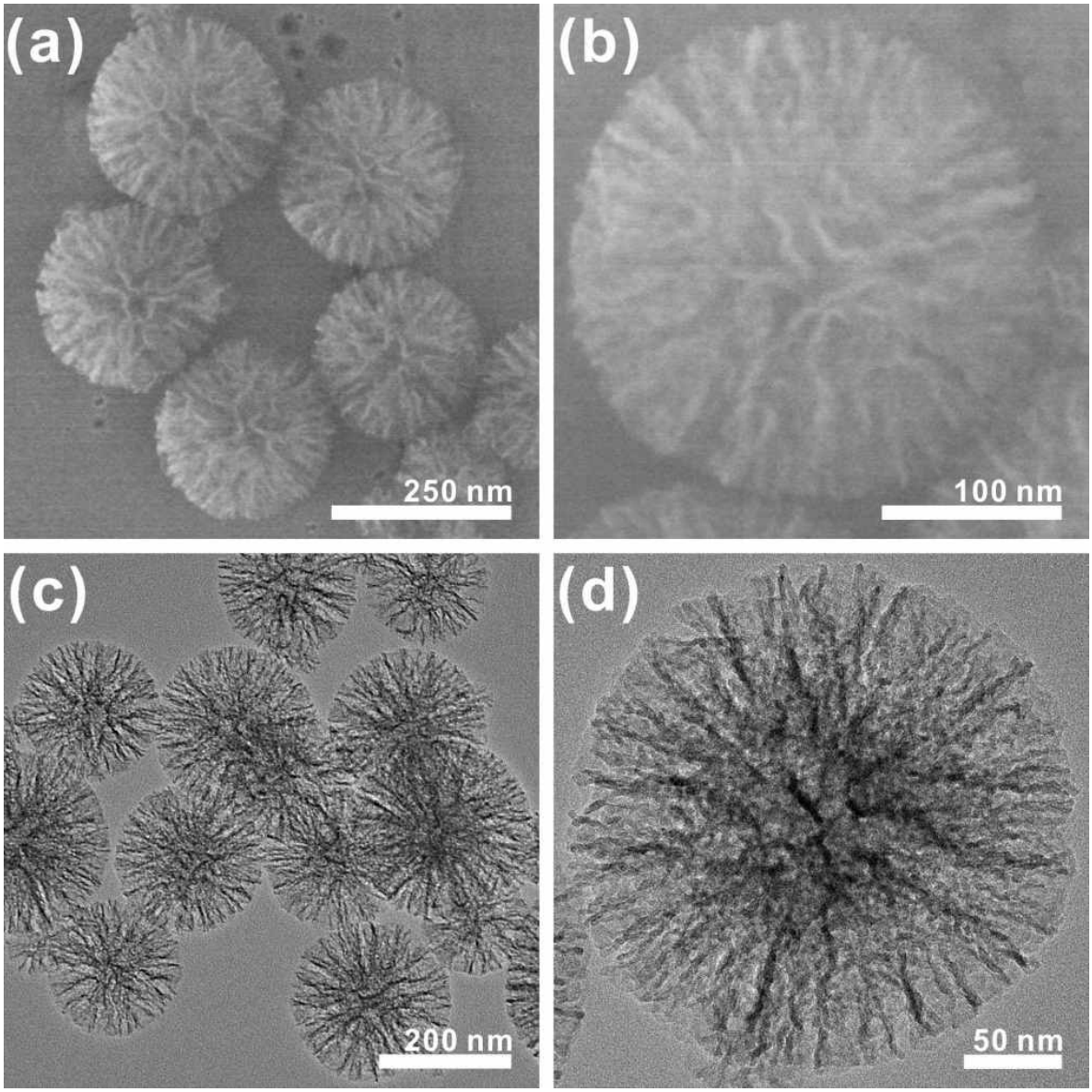

Figure S1. (a, b) SEM and (c, d) TEM images of DFNS.

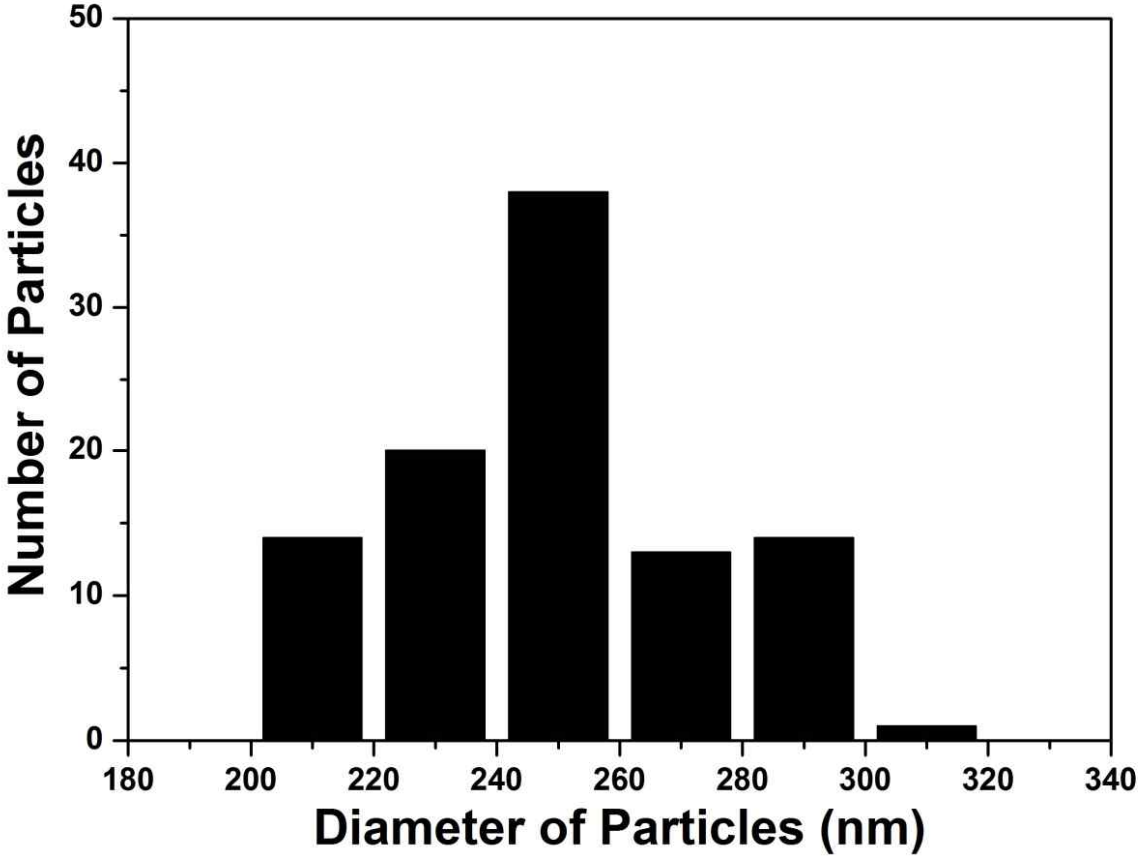

Figure S2. Size distribution of the DFNS. The average diameter is 250.59 ± 24.78 nm (More than 100 nanoparticles are evaluated).

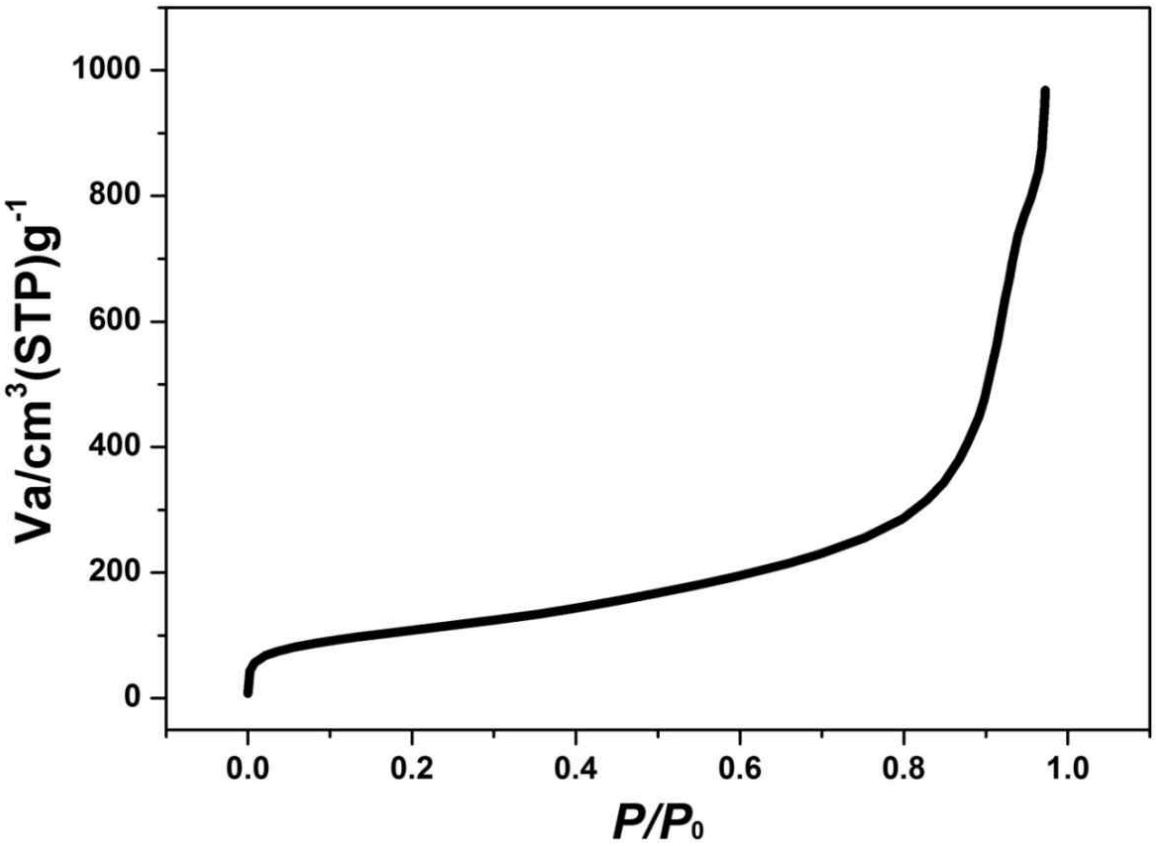

Figure S3. Nitrogen adsorption measured at 77 K of the DFNS. The specific surface area, pore volume, and pore size are 378.48 m^2 g^{-1}, 1.49 cm^3 g^{-1}, and 15.46 nm, respectively.

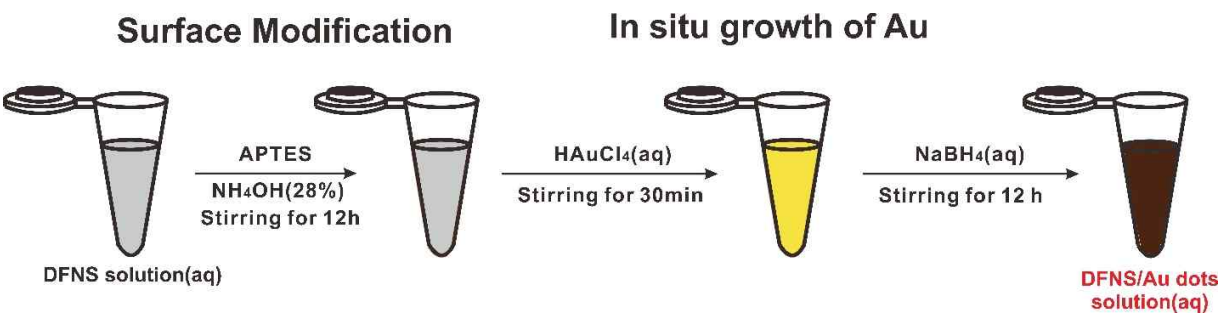

Figure S4. Schematic illustration of synthetic protocol of DFNS/Au dots by surface modification and an *in situ* growth method.

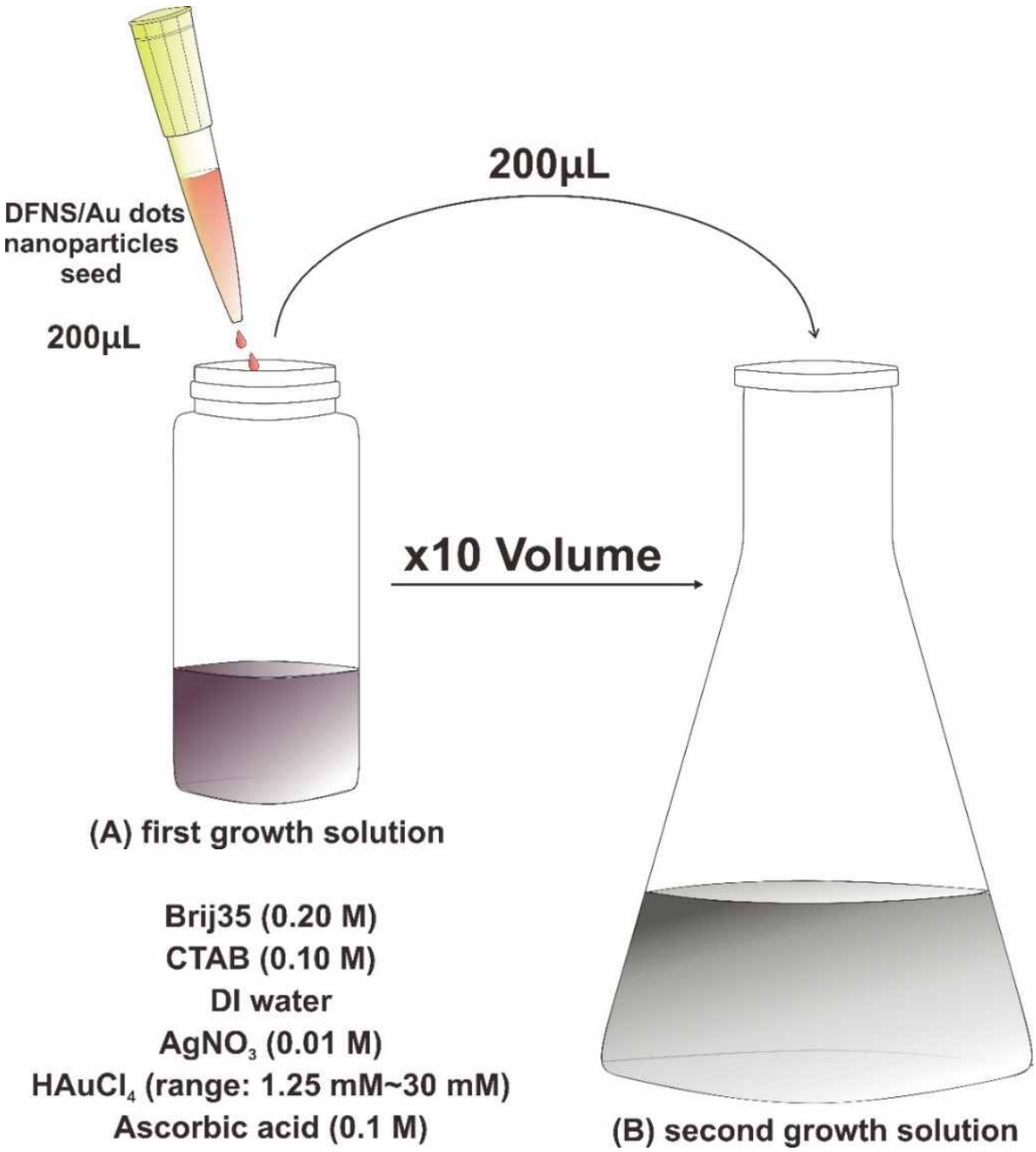

Figure S5. Schematic illustration of the synthesis of the DFNS/Au hybrids by a seed-mediated growth method.

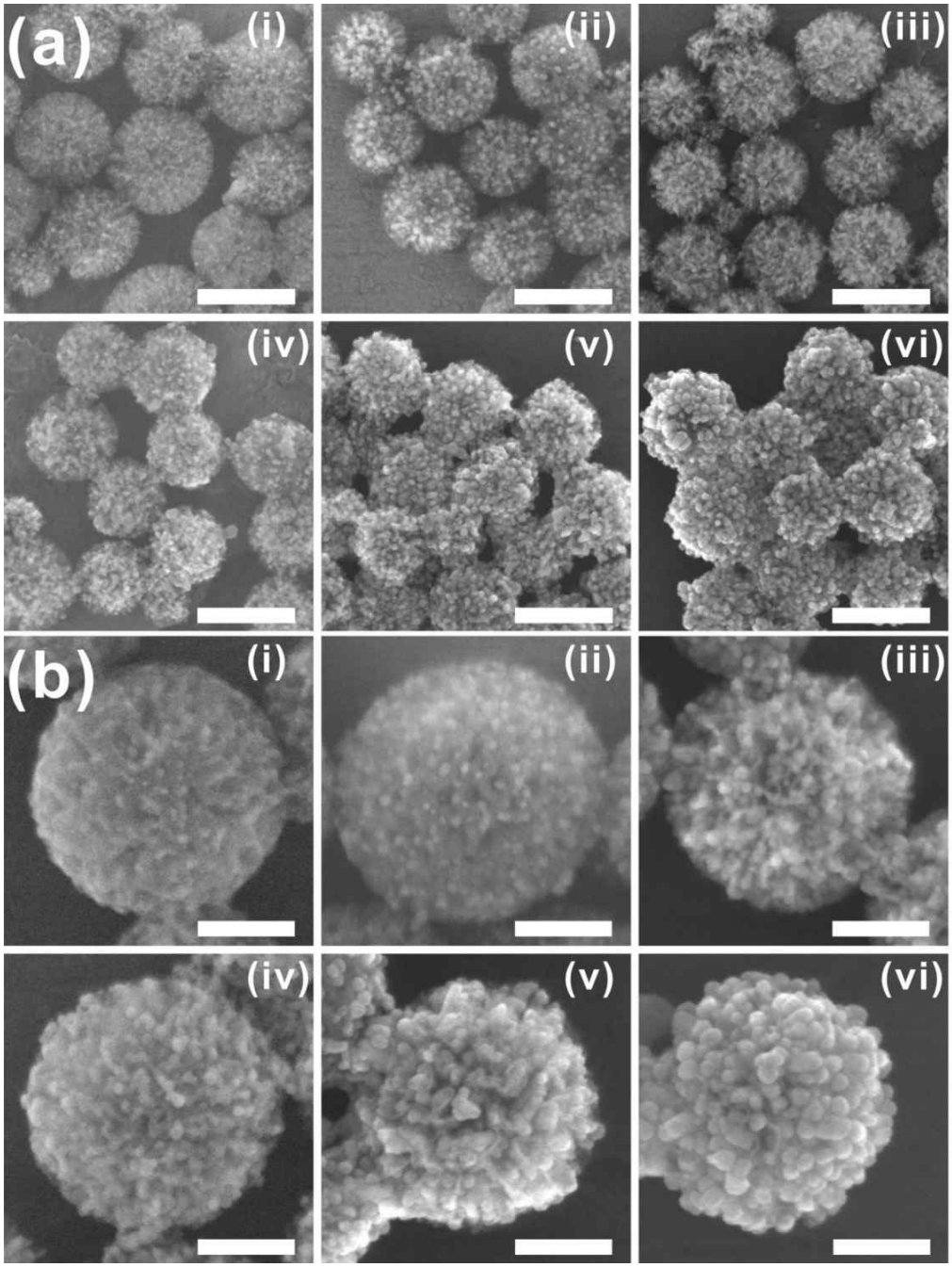

Figure S6. SEM images of DFNS/Au hybrids synthesized using various $HAuCl_4$ (aq) concentrations ((a) a couple of particles, scale bar: 250 nm, (b) a single particle, scale bar: 100 nm): (i) 1.25 mM, (ii) 2.5 mM, (iii) 5 mM, (iv) 10 mM, (v) 20 mM, and (vi) 30 mM $HAuCl_4$ (aq) (the same volume of the second growth solution, 0.8 mL is used in all cases). Based on the synthesis ratio (molar ratio = amount of $HAuCl_4$ in the growth solution/amount of $HAuCl_4$ in the DFNS/Au dots), the reaction ratio can be assigned as (i) 7, (ii) 15, (iii) 30, (iv) 61, (v) 123, and (vi) 246.

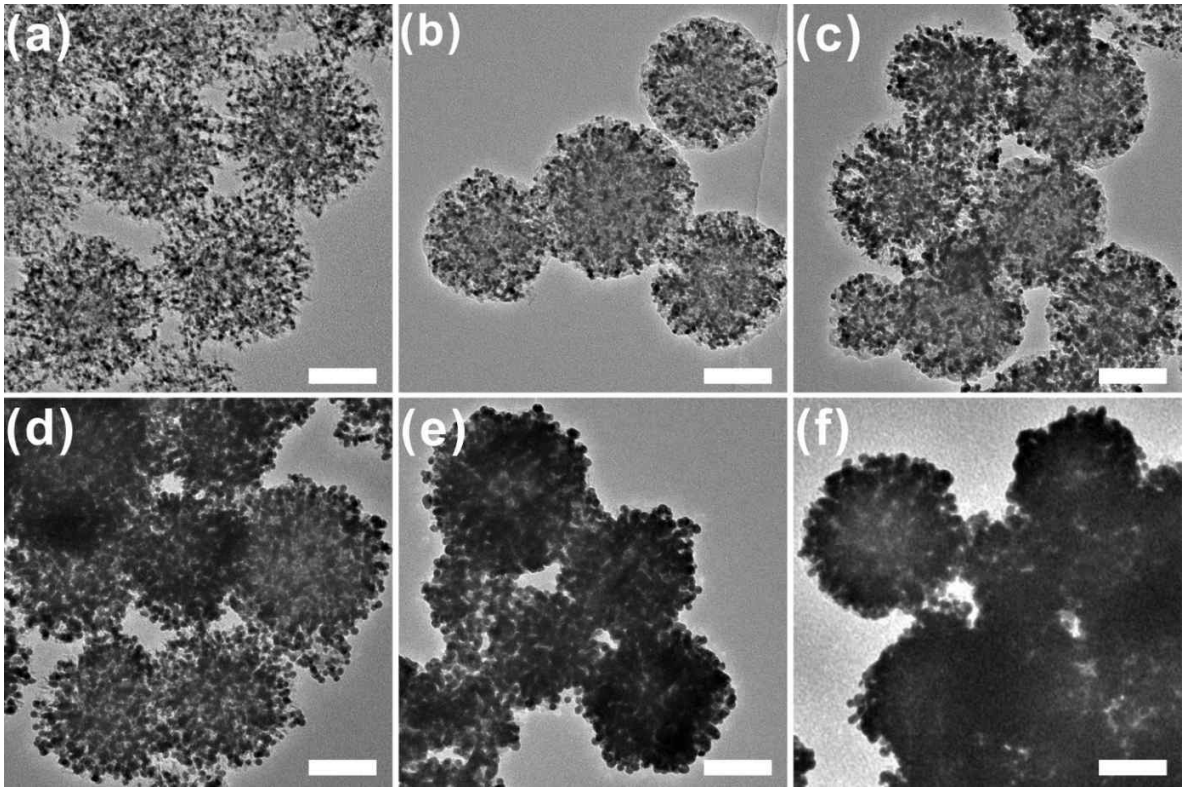

Figure S7. TEM images of DFNS/Au hybrids synthesized using various $HAuCl_4$(aq) concentrations: (a) 1.25 mM, (b) 2.5 mM, (c) 5 mM, (d) 10 mM, (e) 20 mM and (f) 30 mM $HAuCl_4$(aq) (the same volume of the second growth solution, 0.8 mL, was used in each case). Based on the synthesis ratio (molar ratio = amount of $HAuCl_4$ in growth solution/amount of $HAuCl_4$ in the DFNS/Au dots), the reaction ratio can be assigned as (a) 7, (b) 15, (c) 30, (d) 61, (e) 123, and (f) 246. Scale bar: 250 nm.

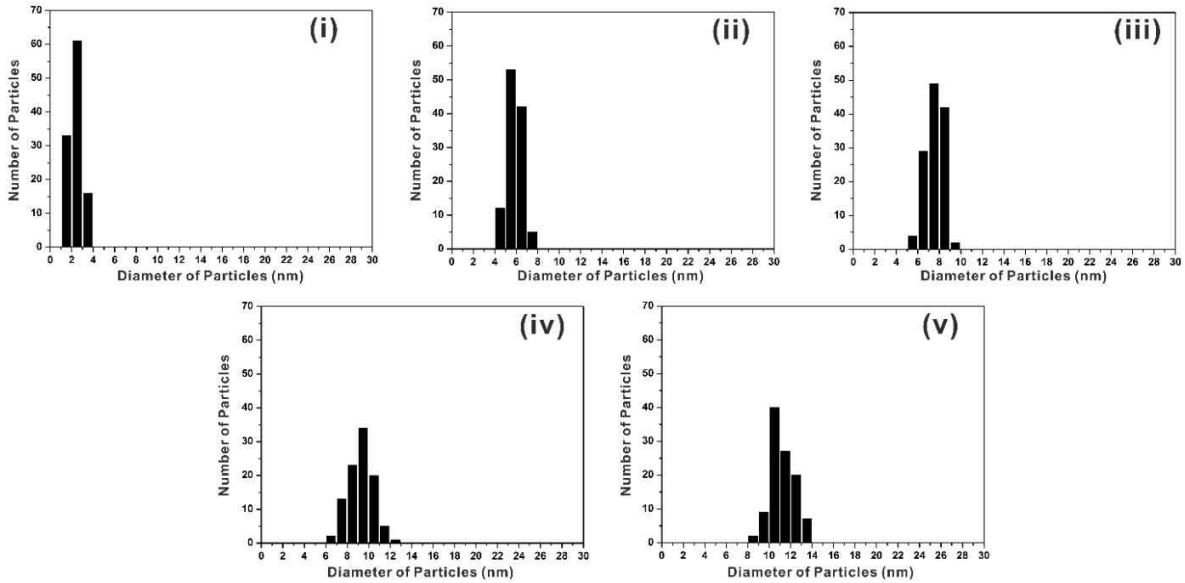

Figure S8. Size distributions of the Au nanodots or nanoparticles in various DFNS/Au NPs. The average diameters are 2.34 ± 0.64 nm ((i) DFNS/Au dots); 5.93 ± 0.76 nm ((ii) ratio: 7); 7.49 ± 0.82 nm ((iii) ratio: 15); 9.25 ± 1.12 nm ((iv) ratio: 30); 11.17 ± 1.14 nm ((v) ratio: 61). More than 100 nanodots or nanoparticles are analyzed in each evaluation.

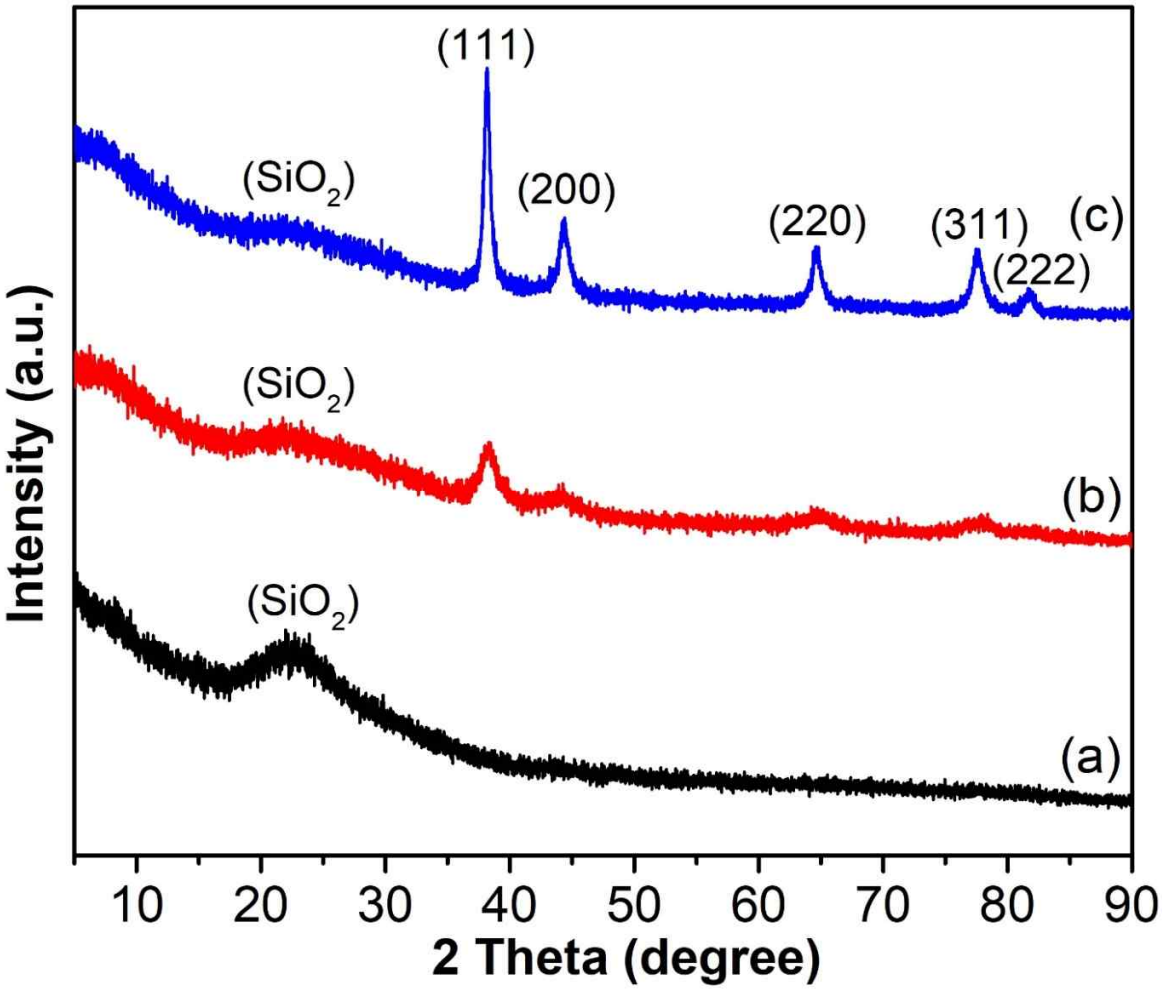

Figure S9. Powder X-ray diffraction (PXRD) patterns of (a) DFNS (black line) and DFNS/Au hybrids synthesized using (b) 5 mM (red line) and (c) 30 mM $HAuCl_4$ (aq) (blue line) (the same volume of the second growth solution, 0.8 mL, is used in all cases). Based on the synthesis ratio (molar ratio = amount of $HAuCl_4$ in the growth solution / amount of $HAuCl_4$ in the DFNS/Au dots), the reaction ratios can be assigned as (b) 30 and (c) 246. Diffraction peaks of 2θ = 38.2, 44.4, 64.8, 77.7, and 81.7 can be assigned to the (111), (200) (220), (311), and (222) reflections.

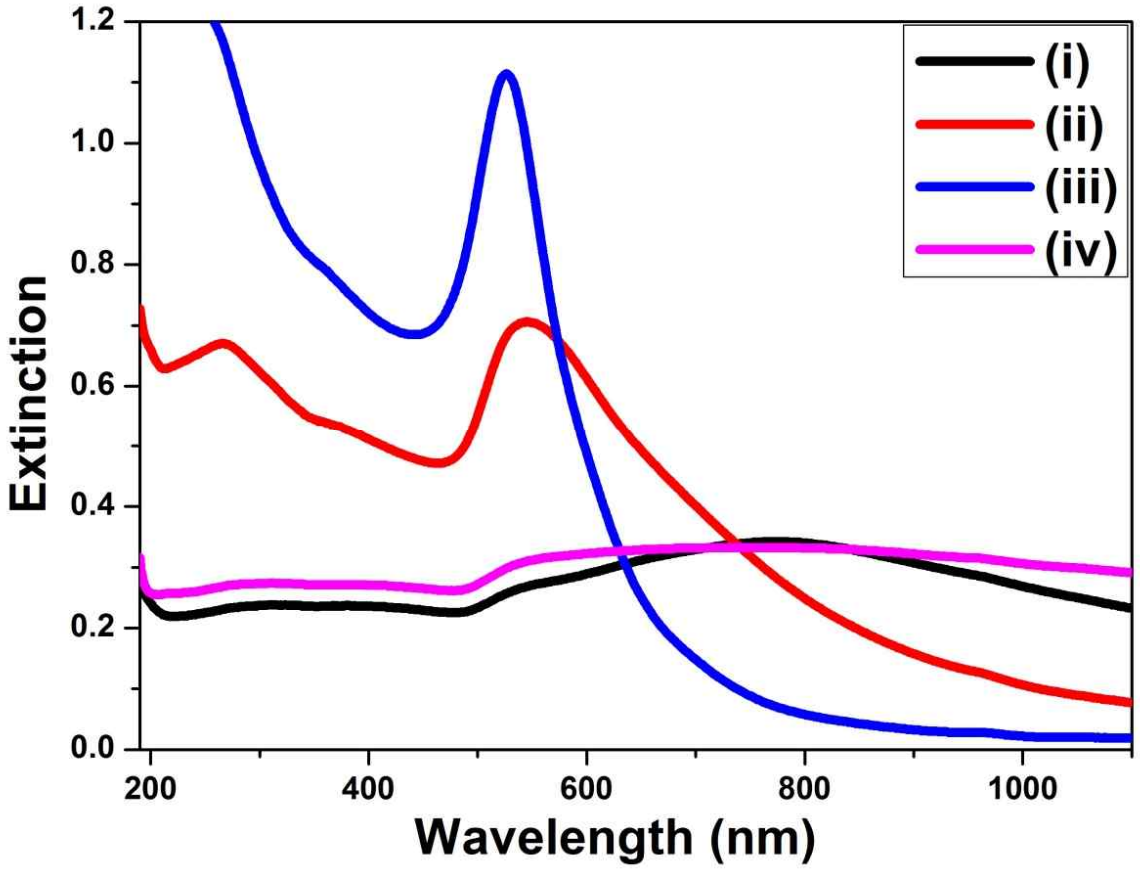

Figure S10. UV-vis spectra of aqueous solutions of DFNS/Au nanosystems synthesized using varying reaction conditions: (i) DFNS/Au layers (ratio: 246, original condition), (ii) without $AgNO_3$ (aq), (iii) without Brij 35, and (iv) without CTAB (The $HAuCl_4$ concentration is 30 mM in each case, other experimental conditions remain the same).

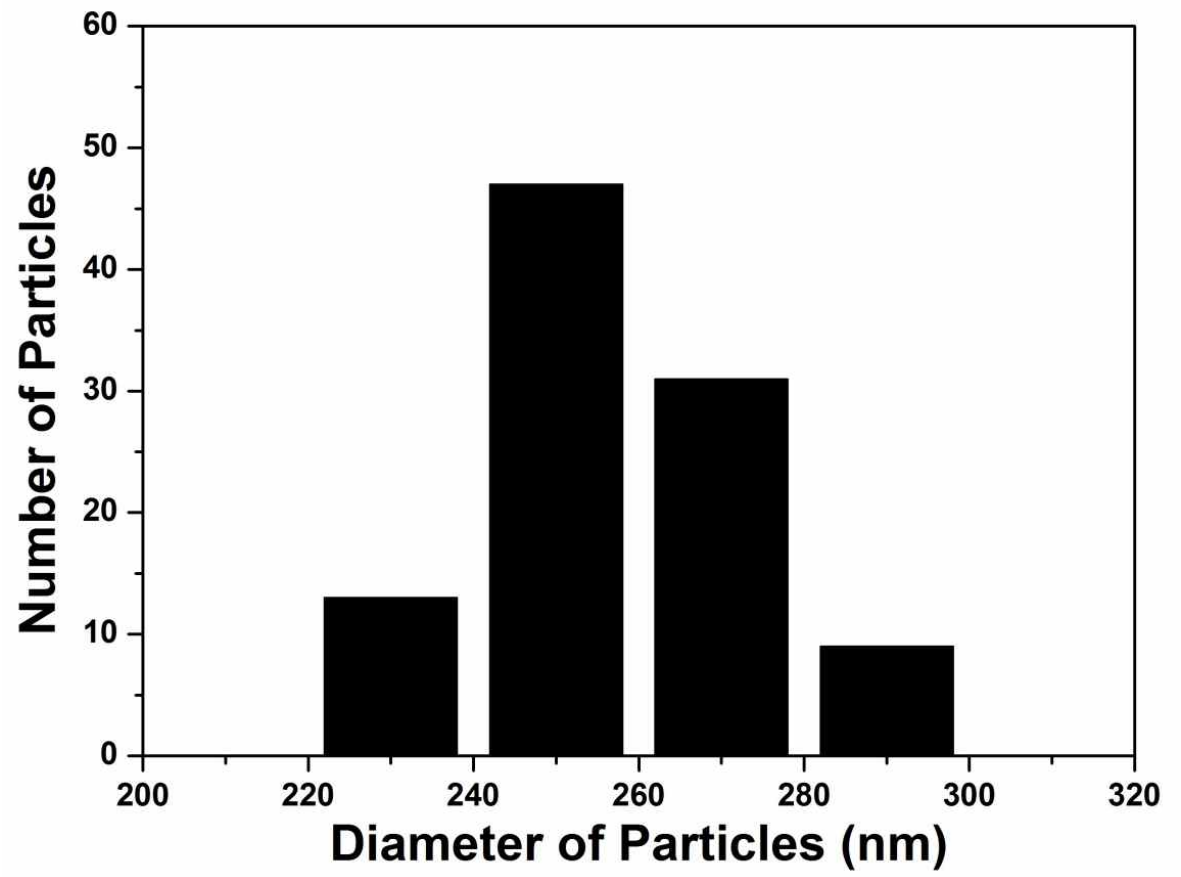

Figure S11. Size distribution of the SNS. The average diameter is 258.12 ± 15.43 nm (More than 100 nanoparticles are evaluated).

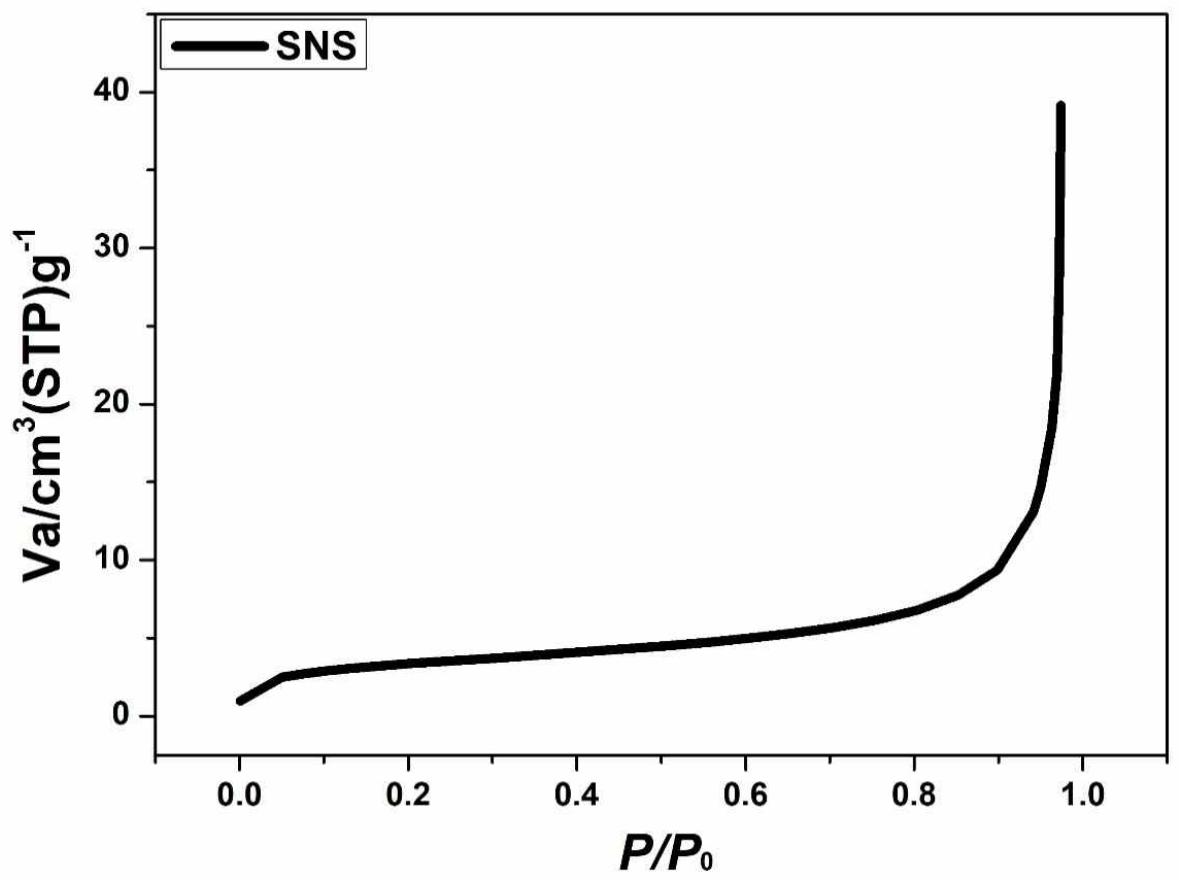

Figure S12. Nitrogen adsorption measured at 77 K of the SNS. The specific surface area and pore volume are 11.55 $m^2 g^{-1}$ and 0.060 $cm^3 g^{-1}$, respectively.

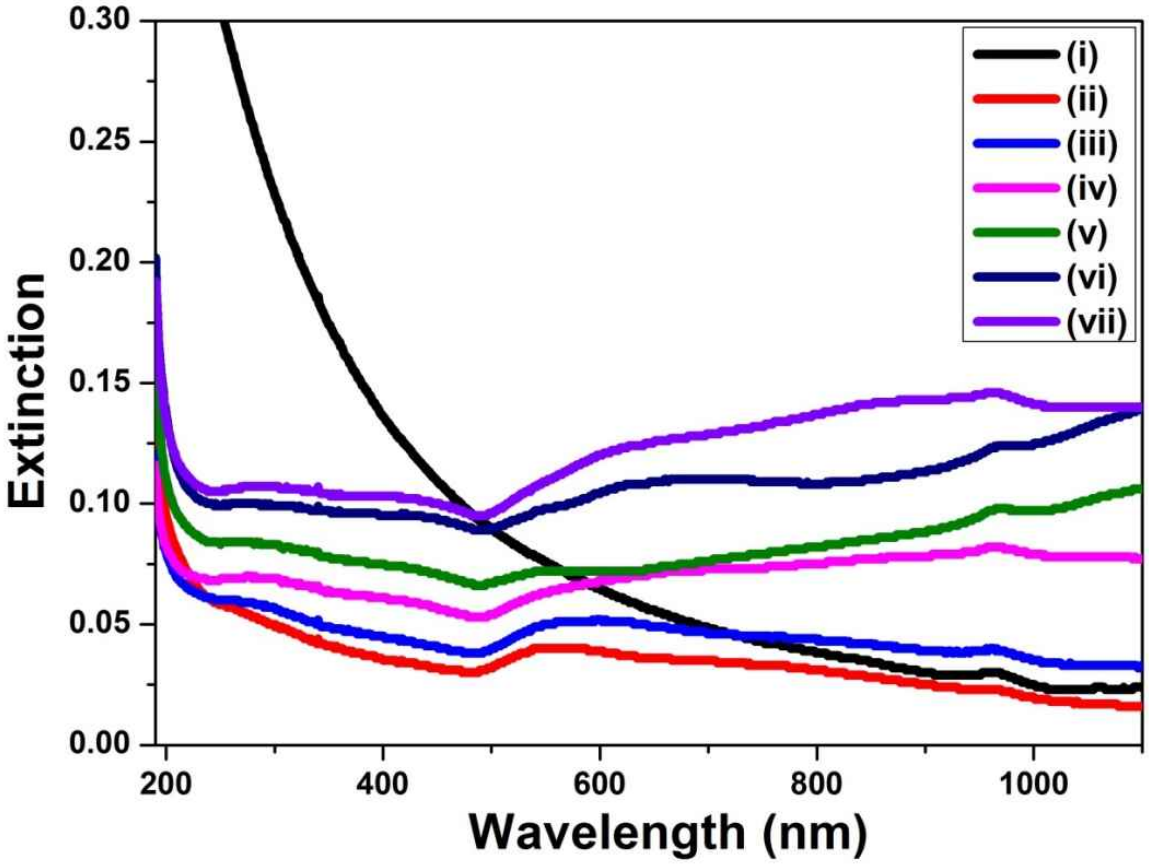

Figure S13. UV-vis spectra of aqueous solutions of SNS/Au hybrids synthesized using various $HAuCl_4$(aq) concentrations: (i) SNS/Au dots, (ii~vii) SNS/Au NPs; (ii) 1.25 mM, (iii) 2.5 mM, (iv) 5 mM, (v) 10 mM, (vi) 20 mM and (vii) 30 mM $HAuCl_4$(aq) (The same volume of the second growth solution, 0.8 mL, is used in each case.

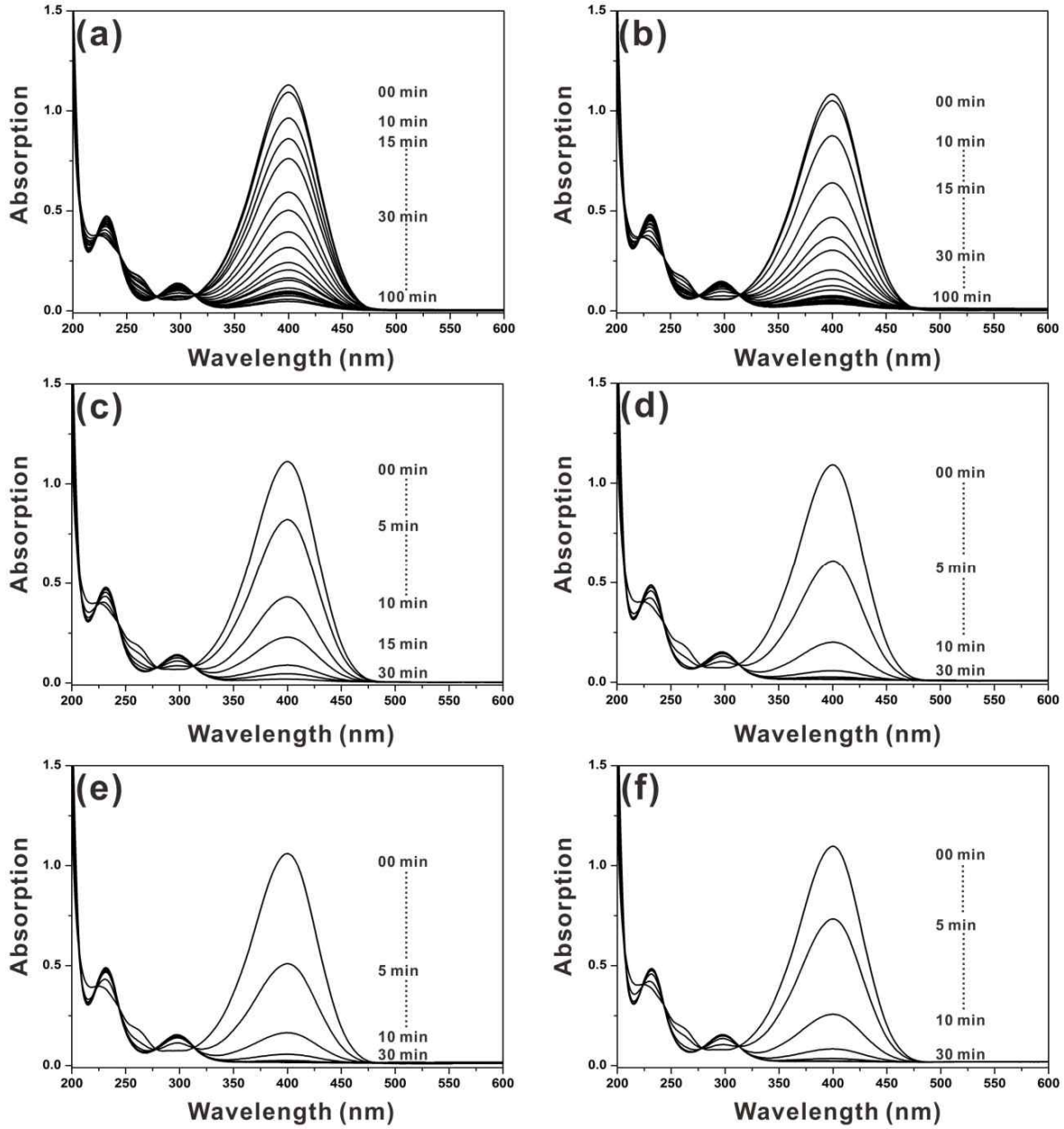

Figure S14. Catalytic reduction of 4-NP using DFNS/Au hybrids with various reaction ratios: (a) 7, (b) 15, (c) 30, (d) 61, (e) 123, and (f) 246.

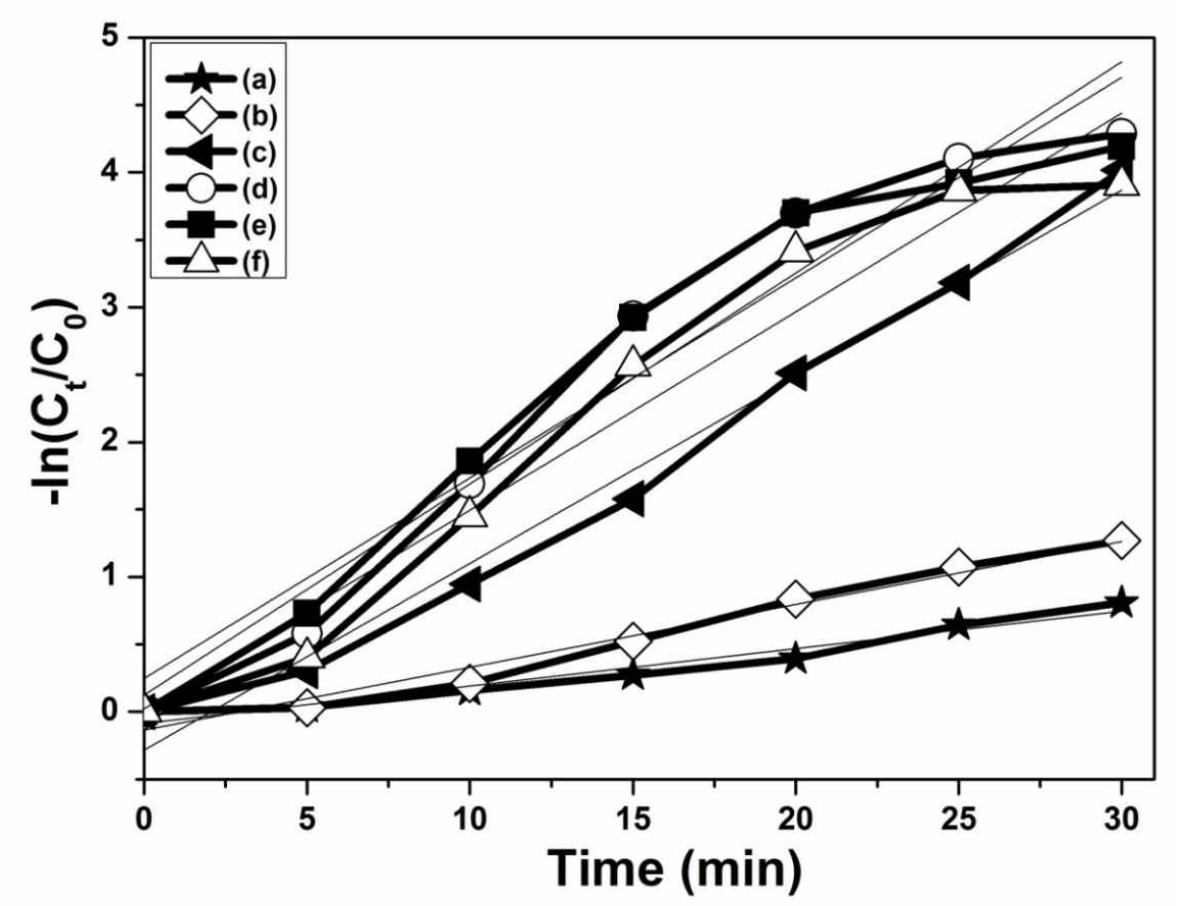

Figure S15. Plot of -ln($C_tC_0^{-1}$) versus time for the reduction of 4-NP using catalysts DFNS/Au hybrids with various reaction ratios: (a) 7, (b) 15, (c) 30, (d) 61, (e) 123, and (f) 246.

Table S1. Conversion rates of 4-NP reduction reaction using different DFNS/Au hybrids (the conversion of 4-NP is calculated as follows: Conversion (%) = $(1 - C_t C_0^{-1}) \times 100$, where C_t is the absorption of 4-NP at a given reaction time, t, and C_0 is the initial absorption by 4-NP at $t = 0$).

Catalyst (Ratio)	*Conversion Rate (30 min, %)*
DFNS/Au hybrids (ratio: 7)	55.49 %
DFNS/Au hybrids (ratio: 15)	71.92 %
DFNS/Au hybrids (ratio: 30)	98.20 %
DFNS/Au hybrids (ratio: 61)	98.63 %
DFNS/Au hybrids (ratio: 123)	98.49 %
DFNS/Au hybrids (ratio: 246)	98.00 %

Table S2. The rate constants of 4-NP reduction reaction using different DFNS/Au hybrids calculated from the slope of the linear fit of $-\ln(C_t C_0^{-1})$ versus time.

Catalyst (Ratio)	*Rate Constant* $(10^{-3}\ min^{-1})$
DFNS/Au hybrids (ratio: 7)	23.8
DFNS/Au hybrids (ratio: 15)	40.3
DFNS/Au hybrids (ratio: 30)	125.3
DFNS/Au hybrids (ratio: 61)	162.3
DFNS/Au hybrids (ratio: 123)	160.0
DFNS/Au hybrids (ratio: 246)	148.3